ESANN 2024 proceedings, European Symposium on Artificial Neural Networks, Computational Intelligence and Machine Learning. Bruges (Belgium) and online event, 9-11 October 2024, i6doc.com publ., ISBN 978-2-87587-090-2. Available from http://www.i6doc.com/en/.

Unveiling Dreams: Moving Towards Automatic Dream Decoding via PSD-Based EEG Analysis and Machine Learning

André Torvestad[1], Mithila Packiyanathan[1],
Luis Alfredo Moctezuma[2*]and Marta Molinas [1]

1- Department of Engineering Cybernetics,
Norwegian University of Science and Technology. Trondheim, Norway

2- International Institute for Integrative Sleep Medicine,
University of Tsukuba. Tsukuba, Ibaraki, Japan

Abstract. Equipping brain-computer interfaces with dream decoding capabilities could be vital in healthcare applications. We used high-density electroencephalogram data from non-rapid eye movement sleep to conduct qualitative analysis employing multivariate empirical mode decomposition and power spectral density (PSD) for preprocessing and machine learning algorithms to distinguish between a dream experience and no experience. Qualitative analysis shows differences between the two classes, especially in the theta and beta bands. We achieve a classification performance of 0.915 in accuracy, 0.851 in AUROC, and 0.715 in kappa with PSD features and extreme gradient boosting classifier.

1 Introduction

Throughout human history, understanding the nature of dreams has been long-sought. In the book of Genesis the Pharaoh sent for all the wise men in Egypt to help him understand the meaning of his dreams [1]. Today, we are on the path of making the Pharaohs long-overdue dream decoder a reality. The goal has transcended deciphering messages from the gods, it now aims to deepens our comprehension of individuals' mental and emotional states.

Research has shown a correlation between dream content and mental health conditions, suggesting that analyzing dream content could be beneficial for the early diagnosis and treatment of various mental disorders [2, 3]. Without any tools for automatic retrieval of dream content while the subject is sleeping, dream content can only be collected by awakening the subject throughout the night. This is detrimental to sleep quality. Automatic decoding of dream content on a sleeping subject would facilitate the collection of dream content for further analysis, to capture early symptoms of mental health conditions. This would allow for earlier treatment and better understanding of the conditions.

Previous research has shown differences in EEG patterns between dream experiences (DE) and no experiences (NE) during non-rapid eye movement (NREM) sleep using power spectral density (PSD) [4–7]. Our work aims to further contribute to the understanding of dreams during NREM sleep from EEG-based analysis and classification, as a step towards the realization of a brain-computer interface (BCI) with dream decoding capabilities.

*This work was partially supported by the Japan Society for the Promotion of Science (JSPS) Postdoctoral Fellowship for Research in Japan: Fellowship ID P22716

ESANN 2024 proceedings, European Symposium on Artificial Neural Networks, Computational Intelligence and Machine Learning. Bruges (Belgium) and online event, 9-11 October 2024, i6doc.com publ., ISBN 978-2-87587-090-2. Available from http://www.i6doc.com/en/.

Here, we present a set of experiments for dream experience and no experience classification based on high-density EEG recordings during NREM sleep. We present a qualitative analysis of sleep EEG with dream experiences versus no experience. To facilitate integration into BCIs, we present classification results utilizing channel subsets derived from qualitative analysis.

2 Materials and Methods

2.1 EEG Dataset

The dataset is presented by Zhang and Wamsley through the DREAM database [8, 9]. It consists of EEG recordings from 28 participants recorded using a 58-electrode cap placed according to the international 10-10 system, a sampling rate of 400 Hz, and a high-pass filter set at 0.1 Hz [5].

Participants were instructed to, whenever awakened, provide a dream report. The reports were verbal descriptions of everything that was going through their mind just before awakening or indicating if they could not recall anything. The awakenings were made during sleep onset, N2 sleep, and REM sleep. Most of the recordings were made on sleep onset during the first hour of the night, which came from sleep stages N1 and N2. One N2 and one REM sleep dream reports were made at least one hour after the last sleep onset report. The N2 and REM reports were separated by a minimum of thirty minutes.

For our experiment, we considered whether the participant reported a DE or NE, and the data collected during the sleep stages N1 and N2. A total of 181 NREM sleep epochs are considered, with 24% labeled NE and 76% as DE. Each epoch lasts 73 seconds before awakening.

2.2 Preprocessing, Power Spectral Density, and Classification

A low-pass filter with cutoff frequency of 45 Hz was applied to avoid high-frequency components in the data (referred to as low-pass filtered). Multivariate empirical mode decomposition (MEMD) was applied to the low-pass filtered data to extract the intrinsic mode functions (IMFs), then the three closest IMFs to the low-pass filtered signal, calculated by Euclidean distance, were selected to reconstruct the EEG signals (referred to as MEMD-filtered).

To increase the number of instances for the classifiers, the IMFs were divided into 0.5-second segments before calculating the PSD; This segment size was selected because it showed the best classification performance.

PSD was calculated from the IMFs for two purposes: *1)* To create a topographic map of the average PSD ratio between the DE and NE reports. *2)* To be used as features for extreme gradient boosting (XGBoost). The convolutional neural network (CNN) EEGNeX was also tested on MEMD-filtered data for comparison [10].

2.3 EEG Channel Selection

After PSD calculation, the 58 EEG channels were ordered based on their PSD values, from highest to lowest. The importance of each channel is calculated as $\frac{PSD(DE)}{PSD(NE)} - 1$. With this, we utilize the distinctions between the classes that have been observed in the topographic maps to define the channel importance both when DE is higher than NE and vice versa.

ESANN 2024 proceedings, European Symposium on Artificial Neural Networks, Computational Intelligence and Machine Learning. Bruges (Belgium) and online event, 9-11 October 2024, i6doc.com publ., ISBN 978-2-87587-090-2. Available from http://www.i6doc.com/en/.

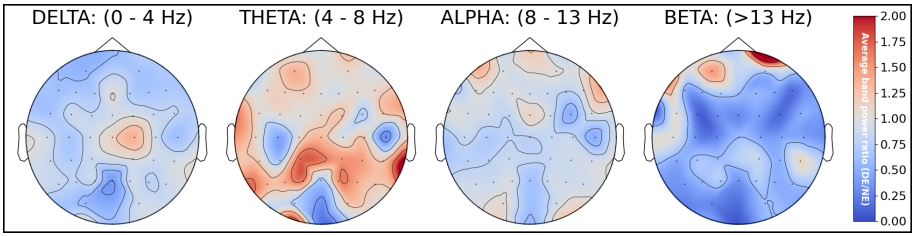

Fig. 1: The average PSD ratio (DE over NE) across all recordings in each channel for IMFs in different frequency bands.

Channel subsets, ranging from one to thirty channels, were created based on channel importance. The n-th subset contains the n most important channels. Classification was performed in each channel subset and evaluated with the kappa metric. The kappa score evaluates performance taking into account expected performance. As expected performance is higher for an imbalanced data set, we chose the kappa metric to evaluate performance on the channel subsets. The kappa score can be interpreted as the agreement between the true data labels and the predicted labels; 0.0-0.2 indicates slight agreement, 0.21-0.40 poor agreement, 0.41-0.60 moderate agreement, 0.61-0.80 substantial agreement, and 0.81-1.00 almost perfect agreement [11].

3 Results

3.1 PSD Ratio between DE and NE with a Topographic Map

The topographic map was created to visualize the difference in PSD between DE and NE in different frequency bands. As each segment is 0.5 seconds long, the frequency resolution is 2 Hz. We iterate through all IMFs within each class and sort them into one of four groups: delta (0 - 4 Hz), theta (4 - 8 Hz), alpha (8 - 13 Hz) or beta and gamma (>13 Hz). The sorting is based on the frequency corresponding to the maximum PSD of the IMF. The grand average of IMFs was calculated for each group in each channel, and then the PSD ratio as the grand average PSD for DE over NE.

The resulting topographic maps are shown in fig. 1. The PSD of DE is higher in the theta band, especially in the parietal and temporal lobes. This is also seen in the frontal lobe in the beta band and in a small central area in the delta. The PSD of NE is generally higher in both the delta and the beta band. This is most prominent in the beta band, which shows the lowest ratio values. The alpha band shows some differences, without any areas being prominent.

3.2 Classification Performance for DE and NE

Three classification configurations are presented: *1)* PSD and XGBoost on MEMD-filtered data, *2)* EEGNeX on MEMD-filtered data, and *3)* XGBoost and PSD on low-pass filtered data. All configurations are validated with five-fold cross-validation, each with a train-test split ratio of 80-20 for each fold. Each train and test set contain segments from all subjects, as the train-test split is performed after the division into 0.5-second segments. The classifications were evaluated using accuracy, F-score,

ESANN 2024 proceedings, European Symposium on Artificial Neural Networks, Computational Intelligence and Machine Learning. Bruges (Belgium) and online event, 9-11 October 2024, i6doc.com publ., ISBN 978-2-87587-090-2. Available from http://www.i6doc.com/en/.

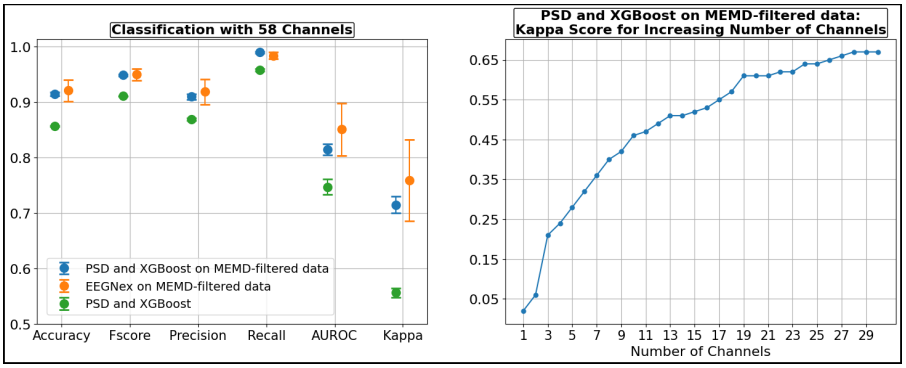

Fig. 2: Classification performance under different configurations: *Left)* XGBoost and PSD on MEMD-filtered data. EEGNeX on MEMD-filtered data. XGBoost and PSD on low-pass filtered data. *Right)* The kappa score evaluated on channel subsets with an increasing number of channels, sorted by highest PSD ratio difference from 1 across all frequency bands.

precision, recall, area under the receiver operating characteristic curve (AUROC), and kappa.

We also present the kappa score from XGBoost and PSD on MEMD-filtered data on channel subsets with an increasing number of channels, up to thirty channels. The classification performance for each channel subset is validated with a five-fold cross-validation, using a train-test split ratio of 80-20.

Using PSD and XGBoost on MEMD-filtered data results in 0.915 accuracy, 0.949 F-score, 0.910 precision, 0.990 recall, 0.815 AUROC, and 0.715 kappa. With EEGNeX on MEMD-filtered data we obtain 0.921 accuracy, 0.950 F-score, 0.919 precision, 0.984 recall, 0.851 AUROC, and 0.759 kappa. Although the metrics are higher for EEGNeX, the standard deviation is also higher. As visualized in fig. 2, the performance of XGBoost is within the standard deviation of EEGNeX for all metrics, with a smaller standard deviation. Omitting MEMD-filtering with PSD and XGBoost, the performance drops to 0.857 accuracy, 0.911 F-score, 0.869 precision, 0.958 recall, 0.747 AUROC, and 0.556 kappa, indicating the importance of MEMD-filtering.

The kappa score with an increasing number of EEG channels shows that the performance increases rapidly in the beginning, before gradually saturating. We obtain a kappa score of 0.46 with the top 10 most important EEG channels, 0.61 with the top 20, and 0.67 with the top 30.

4 Discussion

From our PSD analysis, we observed higher brain activity while dreaming in the theta frequency band, especially over the parietal and temporal lobes. Theta waves are, in awake subjects, related to daydreaming and movement, as well as hyperactivity and impulsivity [12, 13]. The parietal lobe is related to language, spatial recognition, and sensorimotor planning, whereas the temporal lobe is related to vision, hearing, and declarative memory [14]. Dream reports from NREM sleep tend to be more thought-like and less bizarre than dreams from REM sleep - more similar to daydreams [15].

ESANN 2024 proceedings, European Symposium on Artificial Neural Networks, Computational Intelligence and Machine Learning. Bruges (Belgium) and online event, 9-11 October 2024, i6doc.com publ., ISBN 978-2-87587-090-2. Available from http://www.i6doc.com/en/.

Therefore, they resonate well with the observed increase in activity.

The PSD ratio is in general low in the beta frequency band, except for an increase in the frontal lobe and a moderate value in the central-parietal and right temporal lobes. Beta waves are not expected to be prominent during NREM sleep, as they are related to conscious thought, logical thinking, and focus [12]. The reduction of beta waves for DE could indicate a decrease in these processes.

In the delta band, there is, apart from in a spot in the center-right parietal lobe, higher PSD for NE. Similarly to our topographic maps, previous research has found a decrease in PSD for DE during NREM sleep at the source level within the delta frequency band in the parieto-occipital region and in the left brain hemisphere [4, 6].

The observed brain activity linked to DE has been inconsistent in literature [5], having shown both increased and decreased activity in similar areas. We add to this discussion using MEMD-filtered data and show that the observed results can be used for classification.

PSD proves its worth as both a classification feature and as a way to visually understand the differences between DE and NE. PSD combined with XGBoost scores within the standard deviation of the more complex EEGNeX, with both methods achieving accuracy and F-score above 0.9 and kappa above 0.7. PSD also makes it possible to visualize the difference between classes when paired with MEMD.

With PSD and XGBoost, MEMD-filtering improves the performance with 5.8% accuracy, 3.8% F-score, and 15.9% kappa. By selecting the three closest IMFs, and disregarding the others, we removed frequency components from the low-pass filtered data that were possibly negatively affecting the classification performance.

MEMD-filtering is an expensive filtering; we combined it with a relatively simple feature such as PSD to avoid additional expensive computation. Future work should continue to explore simple features paired with MEMD to further investigate the distinction between DE and NE.

A potential limitation could be present in the classifications due to the train-test split regime. In this work we have divided each of the 181 epochs into 0.5-second segments before performing the train-test split. 0.5-second segments from the same epochs are therefore probably present in both the train and the test set. Thus, if some characteristic, like noise, is present in the whole epoch, this would be present in both sets. Although no identical segments are present in both sets, it could lead to a data leakage.

To incorporate dream-decoding capabilities in a BCI, high-performance with a reduced channel subset is required. To achieve a substantial agreement, i.e. kappa score between 0.61-0.8, 19 channels are needed.

Dream reports collected from REM sleep differ from those collected from NREM sleep [15]. We analyze the differences between DE and NE in NREM sleep, and therefore an analysis of REM dream reports is necessary to further understand the nature of dreams.

References

[1] King James Bible Online. Genesis 41:8, n.d. Available at: `https://www.kingjamesbibleonline.org/Genesis-41-8` (Accessed: 05-05-2024).

[2] Tore A. Nielsen, Luc Laberge, Jean Paquet, Richard E. Tremblay, Frank Vitaro, and Jacques Montplaisir. Development of Disturbing Dreams During Adolescence and Their Relation to Anxiety Symptoms. *Sleep*, 23(6):1–10, September 2000.

ESANN 2024 proceedings, European Symposium on Artificial Neural Networks, Computational Intelligence and Machine Learning. Bruges (Belgium) and online event, 9-11 October 2024, i6doc.com publ., ISBN 978-2-87587-090-2. Available from http://www.i6doc.com/en/.

[3] Marine Ambar Akkaoui, Michel Lejoyeux, Marie-Pia d'Ortho, and Pierre A. Geoffroy. Nightmares in Patients with Major Depressive Disorder, Bipolar Disorder, and Psychotic Disorders: A Systematic Review. *Journal of Clinical Medicine*, 9(12):3990, December 2020.

[4] Francesca Siclari, Benjamin Baird, Lampros Perogamvros, Giulio Bernardi, Joshua J. LaRocque, Brady Riedner, Melanie Boly, Bradley R. Postle, and Giulio Tononi. The neural correlates of dreaming. *Nature Neuroscience*, 20(6):872–878, June 2017. Number: 6 Publisher: Nature Publishing Group.

[5] Jing Zhang and Erin J. Wamsley. EEG predictors of dreaming outside of REM sleep. *Psychophysiology*, 56(7):e13368, 2019.

[6] Serena Scarpelli, Aurora D'Atri, Anastasia Mangiaruga, Cristina Marzano, Maurizio Gorgoni, Cinzia Schiappa, Michele Ferrara, and Luigi De Gennaro. Predicting Dream Recall: EEG Activation During NREM Sleep or Shared Mechanisms with Wakefulness? *Brain Topography*, 30(5):629–638, September 2017.

[7] Luis Alfredo Moctezuma, Felix Ipanaque, Marta Molinas, and Takashi Abe. Dream emotions identified without awakenings by machine and deep learning from electroencephalographic signals in REM sleep. In *2023 IEEE International Conference on Metrology for eXtended Reality, Artificial Intelligence and Neural Engineering (MetroXRAINE)*, pages 444–449. IEEE, 2023.

[8] Erin Wamsley, Jing Zhang, and Megan Collins. Zhang & Wamsley 2019 Final. 3 2023.

[9] William Wong, Thomas Andrillon, Nicolas Decat, Rubén Herzog, Valdas Noreika, Katja Valli, Jennifer Windt, and Naotsugu Tsuchiya. The DREAM database. 2 2024.

[10] Xia Chen, Xiangbin Teng, Han Chen, Yafeng Pan, and Philipp Geyer. Toward reliable signals decoding for electroencephalogram: A benchmark study to EEGNeX. *Biomedical Signal Processing and Control*, 87:105475, January 2023.

[11] J. Richard Landis and Gary G. Koch. The Measurement of Observer Agreement for Categorical Data. *Biometrics*, 33(1):159–174, 1977. Publisher: [Wiley, International Biometric Society].

[12] Priyanka A. Abhang, Bharti W. Gawali, and Suresh C. Mehrotra. Chapter 3 - Technical Aspects of Brain Rhythms and Speech Parameters. In Priyanka A. Abhang, Bharti W. Gawali, and Suresh C. Mehrotra, editors, *Introduction to EEG- and Speech-Based Emotion Recognition*, pages 51–79. Academic Press, January 2016.

[13] Zahra M. Aghajan, Peter Schuette, Tony A. Fields, Michelle E. Tran, Sameed M. Siddiqui, Nicholas R. Hasulak, Thomas K. Tcheng, Dawn Eliashiv, Emily A. Mankin, John Stern, Itzhak Fried, and Nanthia Suthana. Theta Oscillations in the Human Medial Temporal Lobe during Real-World Ambulatory Movement. *Current Biology*, 27(24):3743–3751.e3, December 2017.

[14] Khalid H. Jawabri and Sandeep Sharma. Physiology, Cerebral Cortex Functions. In *StatPearls*. StatPearls Publishing, Treasure Island (FL), 2024.

[15] Robert Stickgold and Erin J. Wamsley. Chapter 48 - why we dream. In Meir Kryger, Thomas Roth, and William C. Dement, editors, *Principles and Practice of Sleep Medicine (Sixth Edition)*, pages 509–514.e4. Elsevier, sixth edition edition, 2017.